VNU Journal of Science: Mathematics – Physics, Vol. 30, No. 2 (2014) 59-67

Optical Properties of Anatase and Rutile TiO_2:Cr^{3+} Powders

Trinh Thi Loan*, Nguyen Ngoc Long

Faculty of Physics, Hanoi University of Science, 334 Nguyen Trai, Thanh Xuan, Hanoi, Vietnam

Received 09 January 2014
Revised 18 March 2014; Accepted 19 May 2014

Abstract: Anatase TiO_2 powders doped with 0.5, 1.0, 4.0 and 10 mol% Cr^{3+} have been prepared by hydrothermal method. The Cr^{3+} concentration and annealing effects on crystalline structure, absorption and photoluminescent spectra of the synthesized samples have been investigated. The band gap energy of anatase and rutile TiO_2:Cr^{3+} powders with different dopant contents has been determined. Urbach energies (E_u) characterized for the structural disorder in the anatase and rutile TiO_2 host lattice doped with Cr^{3+} ions also have been calculated with different impurity concentrations. At low annealing temperature ($\leq$ 600 ^oC), the samples exhibited anatase phase and the photoluminescent spectra consisted of sharp peaks related to the $^2E(^2G) \rightarrow {}^4A_2(^4F)$ transitions of ions Cr^{3+} in strong octahedral field. At high annealing temperature (1100 ^oC), the samples exhibited rutile phase and the photoluminescent spectra had a broad emission band, which was assigned to the $^4T_1(^4F) \rightarrow {}^4A_2(^4F)$ transitions within the Cr^{3+} ions in weak octahedral field.

Keywords: Anatase and rutile TiO2, Hydrothermal method, Absorption and Photoluminescent spectra.

1. Introduction

Over recent decades, the synthesis and characterization of TiO_2 materials have received significant attention because of their excellent properties and wide range of potential applications. TiO_2 is relatively cheap material exhibiting nontoxicity, high stability against corrosion, self-cleaning and strong oxidation ability. It has used in important areas such as solar energy, photocatalysis, photocells, hydrogen storage, and chemical gas sensors [1-5]. Pure TiO_2 is a large band gap semiconductor, namely 3.23 eV (indirect band gap) for anatase and 3.06 eV (direct band gap) or 3.10 eV (indirect band gap) for rutile [6]. Therefore, TiO_2 does not efficiently to absorb visible light (photon energy ~ 1.7 - 3.1 eV). It is well known that a considerable shift of the absorption threshold of TiO_2 towards visible spectrum can be reached by doping TiO_2 with certain metals (Cr, Fe, Co, Sb, Eu) or nonmetals (N, C, F, S) [4,7-9].

The optical properties of Cr^{3+} ions located in octahedral coordination of the materials such as spinel [10-13], ruby [14-16] and magnesium oxide [17-19] have been extensively researched.

* Corresponding author. Tel.: 84-904367699.
Email: loan.trinhthi@gmail.com

Whereas, the optical properties of Cr^{3+}-doped TiO_2 were not much studied [20-22]. In this work we studied the effect of Cr^{3+} dopant concentration and heat-treating temperature on the structure and band gap of the TiO_2. In particular, the luminescence properties of Cr^{3+} ions in anatase and rutile TiO_2 host crystalline samples were investigated.

2. Experimental

The anatase TiO_2:Cr^{3+} powders with different dopant contents have been prepared by hydrothermal method. The powders were prepared from anatase TiO_2 powders, $Cr(NO_3)_3$ and NaOH aqueous solutions. Firstly, 1 g of TiO_2 was dispersed in 100 ml of 10 M solution of NaOH, followed by steady stirring for 30 min. Then, an appropriate quantity of 0.02 M solution of $Cr(NO_3)_2$ was added to the above solution, followed by continuous steady stirring. TiO_2 powder and $Cr(NO_3)_3$ solutions were mixed with mole ratio of (1-x):x. The mixed solution was then transferred into teflon-lined steel autoclave and kept at reaction temperature of 200 ^oC for 24 h. Thereafter, solid material was filtered off, washed with acid HCl, distilled water and ethanol. Following washing, the obtained powders were poured back into teflon-lined steel autoclave with 100 ml distilled water and kept at reaction temperature of 130 ^oC for 12 h. Finally, solid material was filtered off and dried in air at 100 ^oC for 24 h. The resulting powder was annealed at 600 ^oC and 1100 ^oC in air for 3 h.

The crystal structure of the samples was characterized by a Siemens D5005 Bruker, Germany X-ray diffractometer (XRD) with Cu-Kα_1 irradiation (λ = 1.54056 Å). Diffuse reflection spectroscopy measurements were carried out on a VARIAN UV-VIS-NIR Cary-5000 spectrophotometer. The Kubelka-Munk function, F(R), was considered proportional to the absorption coefficient. The function F(R) was calculated using the equation: $F(R) = \frac{(1-R)^2}{2R} = \frac{K}{S}$, where R, K and S are the reflection, the absorption and the scattering coefficient, respectively [6]. The spectra were recorded at room temperature in the wavelength region of 300 - 800 nm. Photoluminescence (PL) spectra and photoluminescence excitation (PLE) spectra were measured at room temperature using a Fluorolog FL3-22 Jobin Yvon Spex, USA spectrofluorometer with a xenon lamp of 450 W being used as an excitation source.

3. Results and discussion

The XRD patterns of TiO_2 powders doped with 4 and 10 mol% Cr^{3+} before and after being annealed at 600 and 1100 ^oC for 3 h in air are presented in Fig. 1. Anatase and rutile phases were identified according to the JCPDS card 04-0447 and 21-1276, respectively. As shown in this figure, all the un-annealed samples exhibited a single TiO_2 anatase. Neither characteristic peaks of rutile phase nor those of the Cr^{3+} dopant related phase were observed. Whereas, for the samples annealed at 600 ^oC, the intensity of the characteristic peaks of anatase phase became stronger. In particular, the several additional diffraction peaks characteristic of anatase phase such as (103) and (112) diffraction plane were

observed. This proves that after annealing the samples exhibited better crystallinity. For 4 and 10 mol% Cr^{3+} doped samples, in addition to the diffraction peaks of the anatase phase, some weak peaks of the rutile phase were also observed. At 1000 ^{o}C, only characteristic peaks of rutile phase were detected.

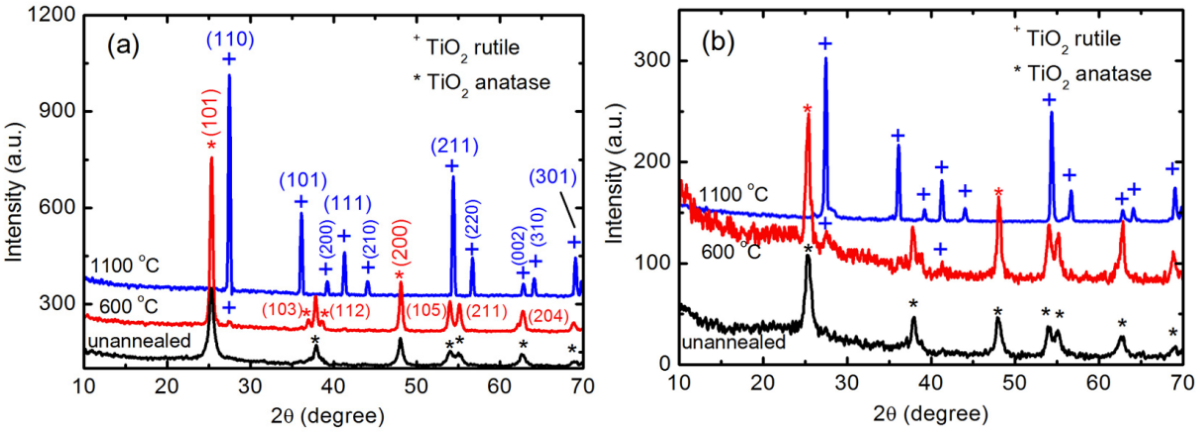

Fig. 1. XRD patterns of the TiO_2 doped with (a) 4 % and (b) 10 mol% Cr^{3+} annealed at different temperatures for 3 h in air.

The diffuse reflectance spectra of Cr^{3+} doped TiO_2 annealed at 600 ^{o}C for 3 h with Cr^{3+} contents of 0.1, 1.0, 4.0 and 10 mol% are shown in Fig. 2a. As shown in this figure, in ranging from 2.0 to 3.5 eV, with increasing Cr^{3+} dopant content, the diffuse reflectance is decreased (absorption is increased). Besides, two weak absorption peaks are observed at 1.65 and 1.73 eV. Fig. 2b shows the Kubelka-Munk functions F(R) of the TiO_2:Cr^{3+} samples obtained from the diffuse reflectance data. On the spectra are seen the sharp absorption outsets in the range 3.3 ÷ 4 eV. In addition, the band absorption located 2.25 – 3.25 eV of Cr^{3+}-doped TiO_2 with dopant contents of 4.0 and 10 mol% are observed, which can be attributed to the charge transfer band $Cr^{3+} \rightarrow Ti^{4+}$ or $^4A_2(^4F) \rightarrow {}^4T_1(^4F)$ d-d transition of Cr^{3+} in octahedral coordination [2, 21]. But two weak absorption peaks at 1.65 and 1.73 eV can be due to $^4A_2(^4F) \rightarrow {}^4T_2(^4F)$ d-d transition of Cr^{3+}. It is known that anatase TiO_2 is an indirect band gap semiconductor [6]. To determine the band gap of anatase TiO_2: Cr^{3+}, the plots of $[F(R)h\nu]^{1/2}$ versus photon energy hν are represented in Fig. 2c. By the line drawn on the liner part of $[F(R)h\nu]^{1/2}$ versus hν curve at $[F(R)h\nu]^{1/2} = 0$ one can receive the band gap values. The band gap of the TiO_2:Cr^{3+} samples with the concentration of 0.1, 1.0, 4.0 and 10 % mol Cr^{3+} to be 3.26, 3.25, 3.16 and 2.96 eV, respectively. Thus, the band gap of anatase TiO_2 is decreased with increasing Cr^{3+} dopant content. In TiO_2, the valence band is composed of O 2p states, and the conduction band is composed of Ti 3d states [23]. The incorporation of Cr^{3+} into the TiO_2 lattice host provides Schottky barrier which facilitates the transfer and/or trapping of electrons from TiO_2 and hence, will appear the charge transfer between the Cr^{3+} ions d-electron and the TiO_2 conduction band. The Cr^{3+} ions could make significant changes on the electronic structure of a crystalline material and thus on the values of the gap energy [24].

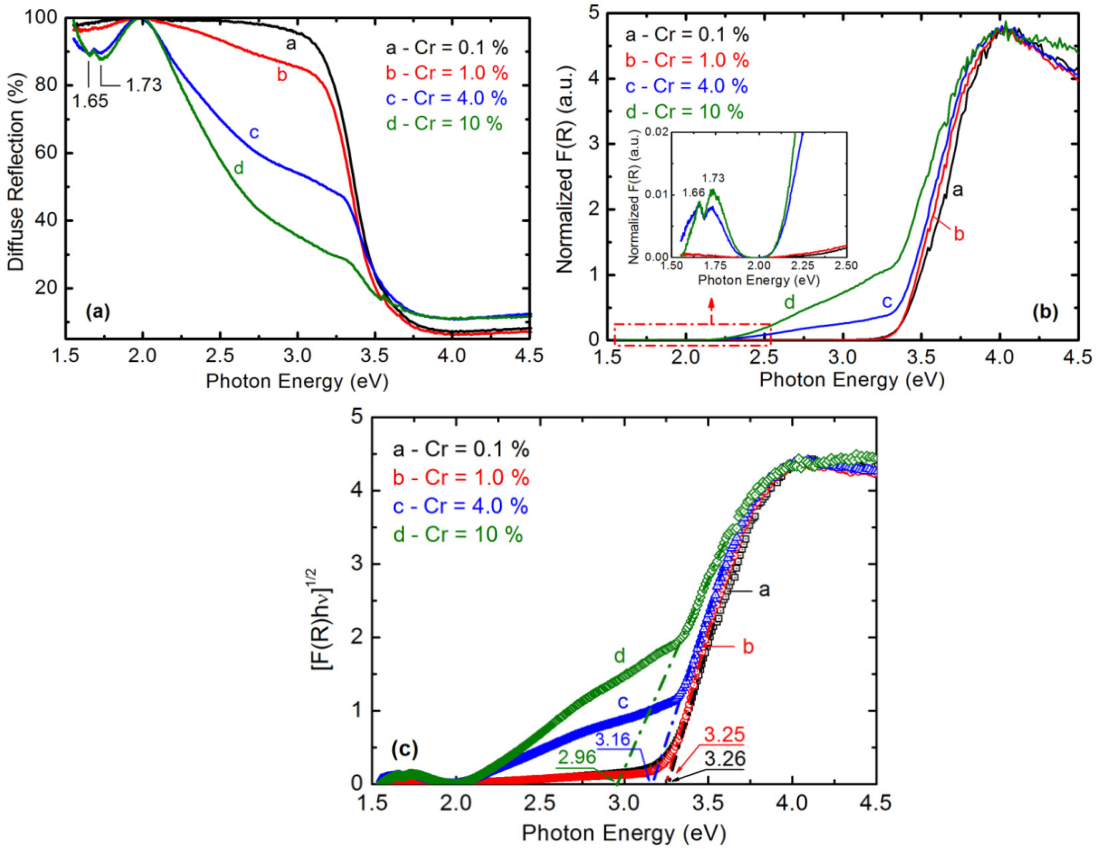

Fig. 2. (a) Diffuse reflectance spectra of Cr^{3+} doped TiO_2 with different Cr^{3+} concentrations annealed at 600 ^oC for 3 h, (b) Kubelka-Munk functions deduced from diffuse reflectance spectra, (c) plots of $[F(R)hv]^{1/2}$ versus photon energy hv.

Urbach energy (E_u) gives a measure of the structural disorder in a material. Effect of Cr dopping induced smearing of the valence and conduction band edges and formation of the Urbach tail is given in Fig. 3.

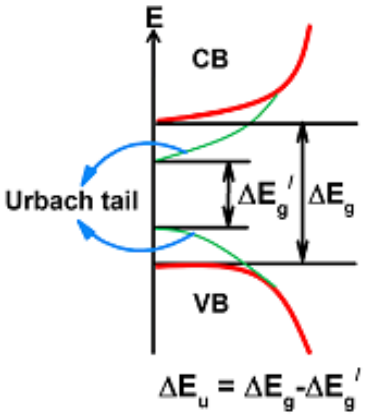

Fig.3. Cr dopping induced smearing of the valence and conduction band edges and formation of the Urbach tail [24]

The equation for E_u was given [24]: $\alpha = \alpha_0 \exp\left(\frac{h\nu}{E_u}\right)$, where α is the absorption coefficient, *hν* is the photon energy. Absorption coefficient α is proportional to F(R), hence, the E_u is calculated by plotting ln[F(R)] versus hν. The reciprocal of slopes of the linear portion, below the optical band gap, gives the value of E_u [25]. For the determination of E_u, plotting of ln[F(R)] versus hν and are presented in Fig. 4. The E_u of the TiO_2:Cr^{3+} samples with the concentrations of 0.1, 1.0, 4.0 and 10 mol% Cr^{3+} to be 62, 75, 583 and 620 meV, respectively. Thus, with increasing Cr^{3+} dopant content, the band gap decreases and the Urbach energy increases.

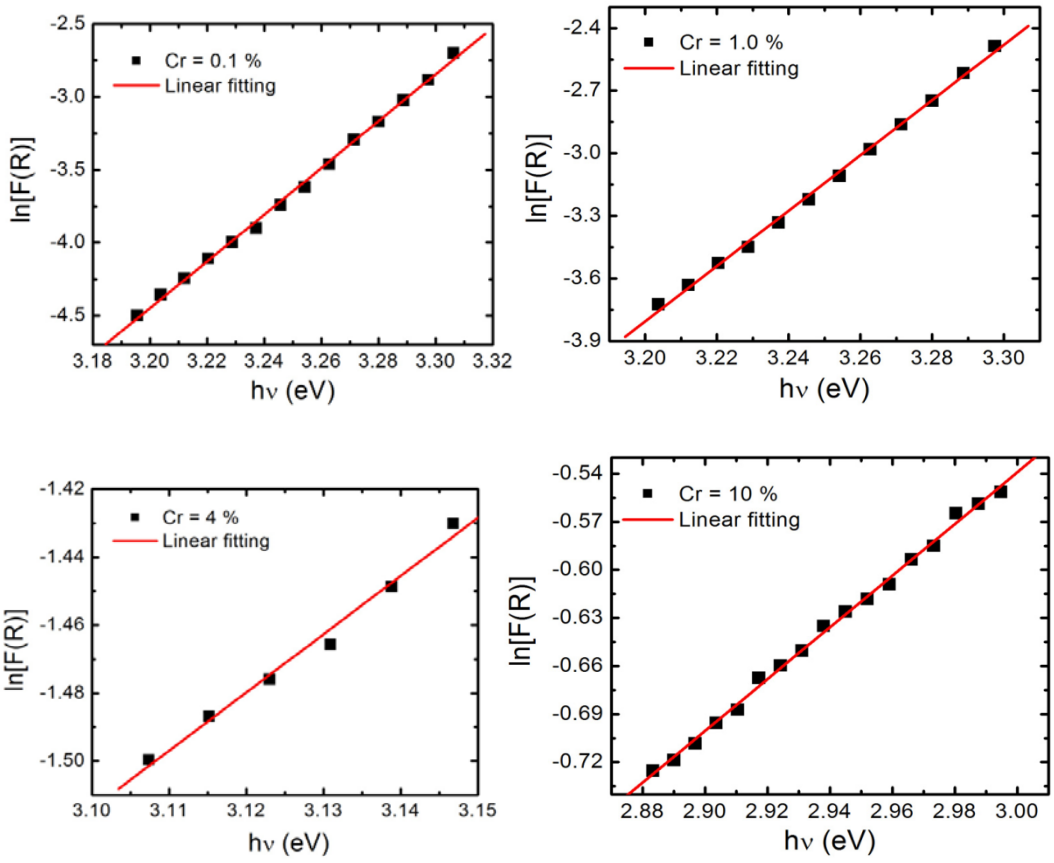

Fig. 4. Plots of ln[F(R)] versus hν for the determination of Urbach energy E_u of Cr^{3+} doped TiO_2 with different Cr^{3+} concentrations annealed at 600 °C for 3 h.

Fig. 5a shows the diffuse reflectance spectra of Cr^{3+}- doped TiO_2 annealed at 1100 °C for 3 h, with dopant contents of 0.1, 0.5, 1.0, 4.0, 8.0 and 10 mol%. It is noted that all the samples annealed at 1100 °C exhibit pure rutile TiO_2 phase. Similar to the anatase phase, in the range from 2.0 to 3.5 eV, with increasing Cr^{3+} content, the diffuse reflectance of Cr^{3+}- doped rutile TiO_2 is decreased. But the quenching of diffuse reflectance by Cr^{3+} doped concentration in rutile phase occurred much more powerful. Kubelka-Munk functions obtained by using diffuse reflectance data of rutile TiO_2:Cr^{3+} with various dopant contents are shown in Fig. 5b. Can be seen that the absorption edge of rutile TiO_2 shifts strongly towards the visible region with increasing Cr^{3+} dopant concentration. In particular, for samples doped with 4.0, 8.0 and 10 mol% Cr, the absorption band around 2.0 - 3.0 eV assigned to the $^4A_2(^4F) \rightarrow {}^4T_1(^4F)$ d-d transition of Cr^{3+}

in octahedral coordination of rutile TiO_2 has become very strong. This absorption band combined with the absorption band of rutile TiO_2 host lattice forming a large absorption range from 2 to 4 eV. Thus, the absorption band of rutile TiO_2 host lattice could be extended considerably towards the visible region by doping host lattice with Cr^{3+}.

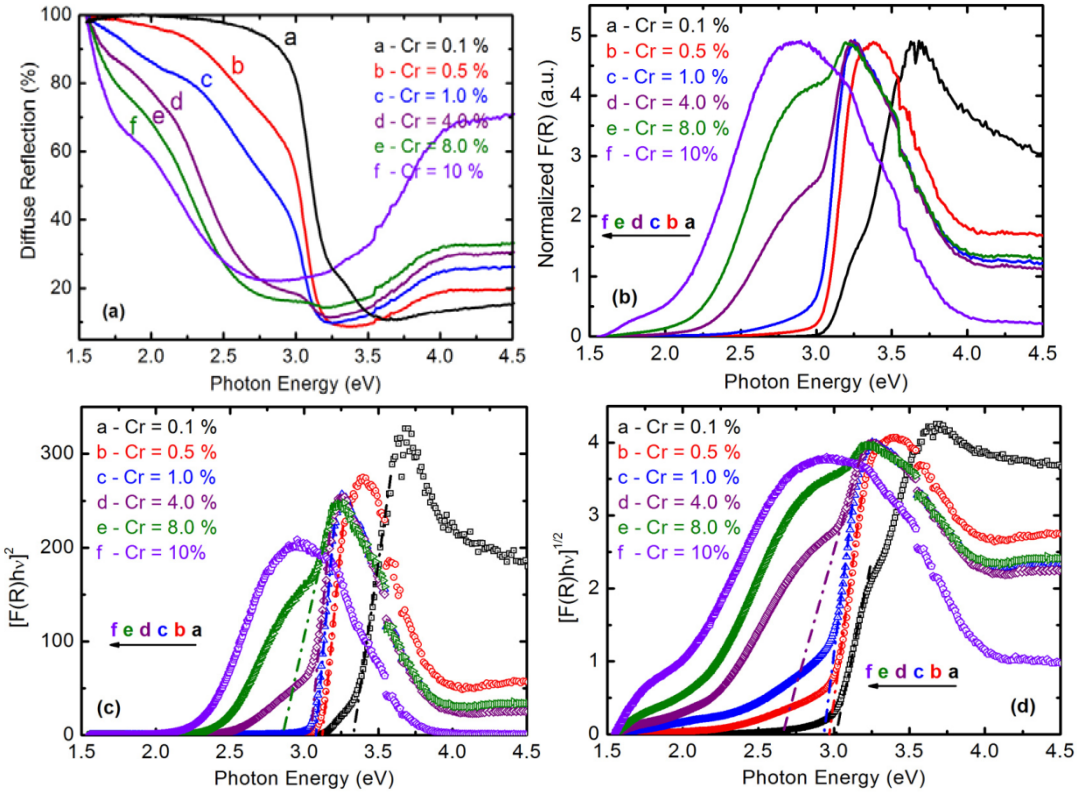

Fig. 5. (a) Diffuse reflectance spectra of Cr^{3+} doped TiO_2 with different Cr^{3+} concentrations annealed at 1100 °C for 3 h, (b) Kubelka-Munk functions deduced from diffuse reflectance spectra, (c) plots of $[F(R)h\nu]^2$ and (d) plots of $[F(R)h\nu]^{1/2}$ versus photon energy hν.

To determine the band gap of rutile TiO_2:Cr^{3+}, the absorption data were fitted to equations for direct and indirect bandgap transitions. The plots of $[F(R)h\nu]^2$ and $[F(R)h\nu]^{1/2}$ versus photon energy hν for a direct and an indirect are represented in Fig. 5c and Fig. 5d, respectively. The band gap values of the rutile TiO_2:Cr^{3+} samples with different dopant contents are shown in Table 1.

Table 1. The direct and indirect band gap of rutile TiO_2:Cr^{3+}.

Cr^{3+} dopant content (mol%)	E_g (eV)	
	Direct band gap	Indirect band gap
0.1	3.34 ± 0,01	3.02 ± 0,01
0.5	3.12 ± 0,01	2.97 ± 0,01
1.0	3.08 ± 0,01	2.93 ± 0,01
4.0	3.04 ± 0,01	2.66 ± 0,01
8.0	2.50 ± 0,01	-

From Table 1 it is noted that with the same of Cr^{3+} dopant concentration, the E_g band gap value for direct transition is larger than that for indirect transition. These results are opposite to that reported by Ref. [6], but in agreement with the calculative results of Ekuma et al [26] where they found a direct band gap of 3.05 eV at the Γ point lager than an indirect band gap of 2.95 eV, form Γ to R point.

Urbach energy E_u of the rutile TiO_2:Cr^{3+} samples with the Cr^{3+} concentrations of 0.1, 0.5, 1.0, 4.0 and 8 mol% is calculated to be 44, 58, 74, 242 and 834 meV, respectively.

Fig. 6a shows the PL spectra of the TiO_2 samples doped with 0.5 mol% Cr^{3+}, heat-treated at 600 ^oC for 3 h, excited by wavelengths 533 nm and 541 nm. Under excitation wavelength of 541 nm, in the spectrum only a peak at 693 nm is observed. But under excitation wavelength of 533 nm, beyond the peak at 693 nm, another weak peak at 685 nm is also observed. As mentioned in the introduction, the optical property of Cr^{3+} ions located in octahedral coordination of TiO_2 host materials was not much studied, but it was extensively studied in other materials such as spinel, ruby and magnesium oxide. The similar PL lines of Cr^{3+} ion were revealed in different host materials, for example, line at about 685 nm in $ZnAl_2O_4$ [10-13], line at 693 nm in Al_2O_3 [14-16] and line at 699 nm in MgO [17-19]. These lines have been assigned to the $^2E(^2G) \rightarrow {}^4A_2(^4F)$ transitions within Cr^{3+} ions located in the strong octahedral field.

Thus, the PL peaks at 685 and 693 nm of the anatase TiO_2 samples doped with 0.5 mol% Cr^{3+} can be related to the same $^2E(^2G) \rightarrow {}^4A_2(^4F)$ transitions as well, but arise from the different Cr^{3+} ions in strong ligand-field. In order to confirm the above-mentioned interpretation, the PLE spectra of the anatase TiO_2 samples recorded at 685 and 693 nm are shown in Fig. 6b. The each PLE spectrum consisted of two excitation bands. The first band in the range of 350 – 500 nm may be attributed to $^4A_2(^4F) \rightarrow {}^4T_1(^4F)$ transitions. Meanwhile the second band in the range of 500 – 600 nm may be assigned to $^4A_2(^4F) \rightarrow {}^4T_2(^4F)$ transitions. It can be clearly seen from Fig. 6b that, in the second excitation band, the excitation peak monitored at 685 nm emission line is 8 nm shifted towards the shorter-wavelength side in comparison with that monitored at 693 nm line. This proves that the PL peaks at 685 and 693 nm arise from different classes of Cr^{3+} ions with different, more or less perturbed short range orders.

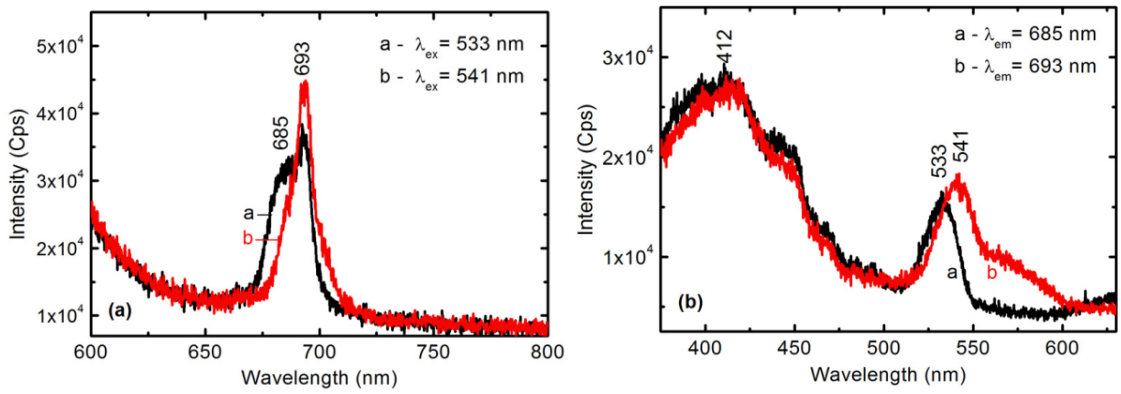

Fig. 6. (a) PL spectra and (b) PLE spectra of the TiO_2 samples doped with 0.5 mol% Cr^{3+}, heat-treated at 600 ^oC for 3 h.

The PL spectrum excited by 533 nm wavelength of the anatase TiO_2 sample doped with 1 mol% Cr^{3+}, heat-treated at 600 °C for 3 h, is similar to that of the sample doped 0.5 mol% Cr^{3+}. However, for the samples doped with 4 and 10 mol% Cr^{3+}, the PL spectra are very different from that of the 0.5 and 1.0 mol% Cr doped samples (Fig. 7a). In the PL spectra excited by 533 nm wavelength, beside peak at 685 nm, is also observed a weaker abroad emission band centered at 815 nm. The reason for this is that in the samples doped with 4 and 10 mol% Cr, beside anatase phase, also exist rutile phase and emission band maybe related to the Cr^{3+} ions in rutile phase. To affirm this assumption, fluorescence spectra of Cr^{3+} doped TiO_2 samples with different concentrations, heat-treated at 1100 ^oC for 3 h were recorded. It is noticed that after heat-treated at 1100 ^oC, all the samples are pure rutile TiO_2 phase. From the PL spectra presented in Fig. 7b, it can be clearly seen that in the PL spectra of all sample, the emission band centered 815 nm is completely dominant. This abroad emission band is assigned to the $^4T_2(^4F) \rightarrow {}^4A_2(^4F)$ transitions within Cr^{3+} ions located in the weak ligand-field. Meanwhile the weak peak at 687 nm is attributed to $^2E(^2G) \rightarrow {}^4A_2(^4F)$ transitions within Cr^{3+} ions located in strong ligand-field sites of rutile TiO_2 host lattice. From Fig. 7b it is also clear that the PL intensity is decreased with increasing Cr concentration. This is a common concentration quenching.

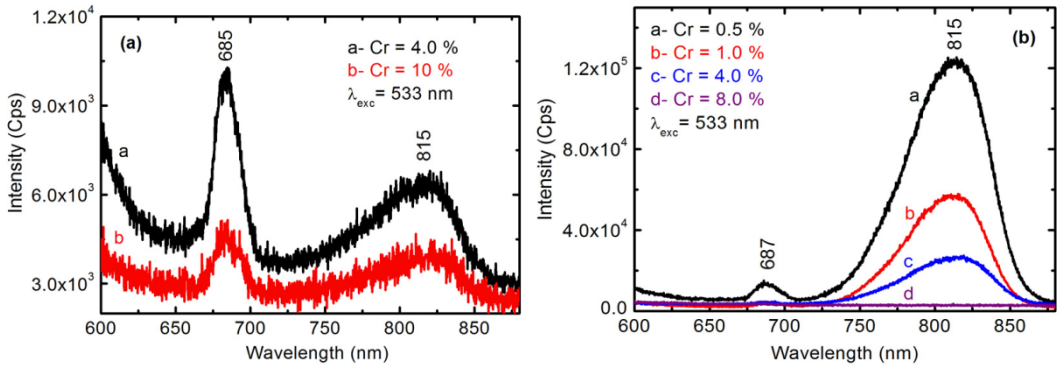

Fig. 7. (a) PL spectra of the TiO_2 samples doped with 4 and 10 mol% Cr^{3+}, heat-treated at 600 ^oC for 3 h, (b) PL spectra of the TiO_2 samples doped with 0.5, 1.0, 4.0 and 8.0 mol% Cr^{3+}, heat-treated at 1100 ^oC for 3 h.

Conclusion

Anatase TiO_2:Cr^{3+} powders with dopant contents ranging from 0.5 to 10 mol% have been successfully synthesized by hydrothermal method. The effect of the Cr^{3+} concentration and heat-treating temperature on the structure, band gap energy, Urbach energy and luminescence properties of the synthesized samples has been studied. The results showed that with increasing Cr^{3+} content, the band gap decreased and the Urbach energy increased for both anatase and rutile TiO_2 host lattice. The PL spectra of TiO_2:Cr^{3+} anatase phase were characterized by sharp peaks at 685 and 693 nm due to $^2E(^2G) \rightarrow {}^4A_2(^4F)$ transitions within Cr^{3+} ions located in strong octahedral field. Meanwhile the PL spectra of TiO_2:Cr^{3+} rutile phase were characterized by a broad luminescence band at 815 nm, which was assigned to the $^4T_2(^4F) \rightarrow {}^4A_2(^4F)$ transitions within the Cr^{3+} ions in weak octahedral field.

Acknowledgment

This work is financially supported by VNU University of Science (Project No. TN-13-03) and Vietnam National University (Project No. QG.14.15). Authors thank the VNU project "Strengthening research and training capacity in fields of Nano Science and Technology, and Applications in Medical, Pharmaceutical, Food, Biology, Environmental protection and climate change adaptation in the direction of sustainable development" for having facilitated the equipment to complete this work.

References

[1] V. Kiisk, I. Sildos, O. Sild and J. Aarik, Optical Materials 27 (2004) 115–118.
[2] J. Zhu, Z. Deng, F. Chen, J. Zhang, H. Chen, M. Anpo, J. Huang, L. Zhang, Applied Catalysis B: Environmental 62 (2006) 329–335.
[3] Honda S. Hafez, M. Saif, James T. McLeskey, Jr., M.S.A. Abdel-Mottaleb, I.S. Yahia, T. Story, and W. Knoff, International Journal of Photoenergy Vol. 2009 Article ID 240402.
[4] W.J. Yin, S. Chen, J.H. Yang, X.G. Gong, Y. Yan, and S.H. Wei, Applied Physics Letters 96 (2010) 221901.
[5] I. Ganesh, A.K. Gupta, P.P. Kumar, P.S.C. Sekhar, K. Radha, G. Padmanabham, and G. Sundararajan, The Scientific World Journal Vol. 2012, Article ID 127326.
[6] S. Valencia, J.M. Marin and G. Restrepo, The Open Materials Science Journal 4 (2010) 9-14.
[7] T. Ikeda, T. Momoto, K. Eda, Y. Mizutani, H. Kato, A. Kudo, and H. Onishi, J. Phys. Chem. C 112 (2008) 1167-1173.
[8] W. Xin, D. Zhu, G. Liu, Y. Hua, and W. Zhou, International Journal of Photoenergy Vol. 2012 Article ID 767905.
[9] W.J. Yin, H. Tang, S.H. Wei, M.M. Al-Jassim, J. Turner, and Y. Yan, Physical Review B 82 (2010) 045106.
[10] [10] C. Koepke, K. Wisniewski, M. Grinberg, D.L. Russell, K. Holliday and G.H. Beall, J. Lumin. 78 (1998) 135-146.
[11] W. Nie, Michel-calendini, C. Linare, G. Boulon and C. Daul, J. Lumin. 46 (1990) 177-190.
[12] D.L. Wood, G.F. Imbusch, R.M. Macfarlane, P. Kisliuk and D.M. Larkin, J. Chem. Phys. 48 (1968) 5255-5263.
[13] Trinh Thi Loan, Le Hong Ha, Nguyen Ngoc Long, VNU Journal of Science, Mathematics –Physics 26 (2010) 37-42.
[14] S.P. Feofilov, A.A. Kaplyanskii, R.I. Zakharchenya, J. Lumin. 66&67 (1996) 349-357.
[15] C. Pan, S.Y. Chen and P. Shen, J. Cryst. Growth 310 (2008) 699-705.
[16] Trinh Thi Loan, Le Hong Ha, Nguyen Ngoc Long, e-J. Surf. Sci. Nanotech. 9 (2011) 531-535.
[17] Trinh Thi Loan, Nguyen Ngoc Long, Nguyen Hung Cuong, Communications in Physics, Vol. 22, No. 3 (2012, 239-246.
[18] D.P. Ma, D.E. Ellis, J. Lumin. 71 (1997) 329-339.
[19] M.B. ONeill, P.N. Gibson and B. Henderson, J. Lumin. 42 (1988) 235-243.
[20] H.G. Kim, J.S. Bae, M.G. Ha, T.E. Hong, J.S. Jin, E.D. Jeong and K.S. Hong, Journal of Korean Physical Society 53, No.5 (2008) 2688-2691.
[21] K.B. Jaimy, S. Ghosh, S. Sankar, K.G.K. Warrier, Materials Research Bulletin 46 (2011) 914-921.
[22] W.Y. Tian, X.Y. Kuang, M.L. Duan, R.P. Chai and C.X. Zhang, Physica B 404 (2009) 4332-4336.
[23] Y. Nagao, A. Yoshikawa, K. Koumot, T. Kato, Y. Ikuhara, H. Ohta, Appl. Phys. Lett. 97 (2010) 172112.
[24] A. Hajjaji, A. Atyaoui, K. Trabelsi, M. Amlouk, L. Bousselmi, B. Bessais, M.A.E. Khakani and M. Gaidi, American Journal of Analytical Chemistry 5 (2014) 473-482.
[25] B. Choudhury, M. Dey and A. Choudhury, International Nano Letters 3 No.1 (2013) 1-8.
[26] C.E. Ekuma, D. Bagayoko, Japanese J. Appl. Phys. 50 (2011) 101103.